

# Impurity Transport Studies on LHD

Yu. IGITKHANOV<sup>1</sup>), P. GONCHAROV, S. SUDO, N. TAMURA, D. KALININA, H. FUNABA, M. YOKOYAMA, S. MURAKAMI<sup>2</sup>), K. KAWAHATA, T. KATO, T. MORISAKI, B. PETERSON, Y. HAKAMURA, H. YAMADA and O. MOTOJIMA.

*National Institute for Fusion Science, Toki 509-5292, Japan*

<sup>1</sup>*Max-Planck-Institut für Plasmaphysik, IPP-EURATOM Ass., Greifswald, Germany*

<sup>2</sup>*Kyoto University, Kyoto 606-850, Japan*

(Received 26 December 2006 / Accepted 20 March 2007)

The preliminary results of impurity transport studies in the Large Helical Device (LHD) by means of a newly developed the Stellarator Impurity Transport code SIT STRAHL [1] are reported. The attenuation of the emission lines from the ionized Ti ions, launched in the plasma edge by means of the TESPEL injector has been numerically simulated and compared with experiment. In the case of low plasma density discharges with positive radial electric field the outward directed neoclassical drift determines a low confinement time of the Ti impurity ions. The SX-ray emission signal can be reproduced fairly well, indicating the neoclassical nature of Ti ions behavior. In the case of high density regimes with a negative value of the electric field the increase of the confinement time seems not to be able to be explained only by neoclassical transport. The importance of radial electric field on impurity behavior is analyzed and impurity accumulation within the externally induced island is simulated.

© 2007 The Japan Society of Plasma Science and Nuclear Fusion Research

Keywords: stellarator neoclassical impurity transport, impurity control, effect of the radial electric field on impurity behavior, TESPEL injection

DOI: 10.1585/pfr.2.S1131

## 1. Introduction

Impurity transport in Large Helical Device (LHD) is an important issue, which can be studied by means of Tracer-Encapsulated Solid PELlet (TESPEL) injection [2]. The tracer amount of Ti is launched into the plasma and the attenuation of the emission lines from the highly ionized states is measured and then numerically simulated by using a newly developed 1-D stellarator impurity transport code SIT STRAHL [1]. The code can be considered as an extension of the tokamak STRAHL code [3] to non-axisymmetric configuration and includes the stellarator specific neoclassical transport coefficients and the ambipolar radial electric field solver. It solves the radial continuity equations for each ionization state of the impurity ions for given background plasma profiles and magnetic configuration. The neoclassical coefficients are based on numerical results from the DKES (Drift Kinetic Equation Solver) code and monoenergetic Monte-Carlo calculations. The transition between the different charge states due to the balance of ionization, recombination and charge exchange is described by using the ADAS (Atomic Data and Analysis Structure) database. Anomalous diffusion and drift models are also incorporated in the code. Here we are reporting the preliminary results of our analysis. The TESPEL signal from Ti impurity radiation is analyzed, indicating the importance of impurity transport in time evolution of

radiation. Here we will emphasize the role of the radial electric field on impurity accumulation. It will be shown that the spatial distribution of impurity ions results from the competition between the radial electric field and the thermal force (which together produce a convective flux), and the diffusive term. The code predicts localization of impurity ions at the radial position, where the convective flux changes from positive to negative with increasing minor radius. It is also confirmed that for typical LHD discharges with  $1/\nu$  dominant neoclassical transport there are no “temperature screening” effect like in tokamak plasmas. Analysis of the TESPEL signal indicates that for high density plasmas anomalous transport of impurity ions must be taken into account; however the neoclassical contribution remains essential for low density discharges. Finally, the effect of an externally induced magnetic island on the impurity screening from the bulk plasma is analyzed.

## 2. Experimental Results and Simulation

Two LHD discharges with low and high central density have been considered. Figure 1 shows the time evolution of the TiK $\alpha$  emission measured by a soft x-ray (SXR) pulse height analyzer viewing a central plasma chord. Titanium pellet was injected into the NBI heated hydrogen plasmas with the central density of  $0.8 \times 10^{19} \text{ m}^{-3}$  and  $T_{e0} = 3 \text{ keV}$  (shot #54018). Figure 3 shows the SXR sig-

author's e-mail: yli@ipp.mpg.de

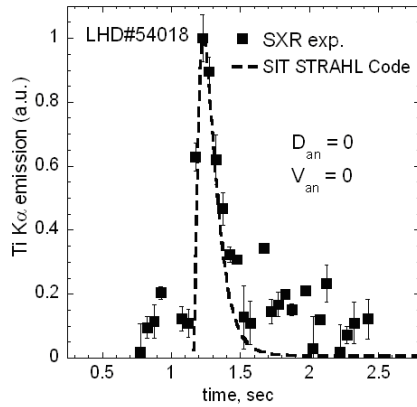


Fig. 1 Time evolution of TiK $\alpha$  emission for the LHD discharge (#54018) with central density  $n(0) = 0.8 \times 10^{19} \text{ m}^{-3}$ . The TESPEL pellet with a titanium tracer is injected at 1.2 s. Result of calculation is shown as a dashed line. Impurity transport is assumed to be purely neoclassical.

nal in the case of higher central density of  $3.4 \times 10^{19} \text{ m}^{-3}$ ,  $T_{e0} = 2.5 \text{ keV}$  (shot #54040) at 1.2 s. In the first case the number of injected Ti atoms was  $2.18 \times 10^{17}$  and pellet was ablated at the radial position  $\rho \sim 0.86$ . In computation the source radial distribution for neutral impurities was taken as a Gaussian with a full width at half maximum (FWHM) of about 4.8 cm. Radial profiles of the time averaged electron density and temperature profiles as measured by interferometer FIR and Tomson scattering, respectively, have been used as input parameters. For neoclassical transport coefficients and the radial electric field calculation the magnetic geometry was specified from equilibrium (VMEC) data with a finite beta correction. This was particularly important in mapping of the major radius to the  $\rho$  value. In the low density case, there is a rapid increase in the TiK $\alpha$  emission signal, followed by a more gradual decay down back to the pre-injection level. This indicates that for this type of discharge the titanium ions readily leave the plasma and there is no accumulation in the centre. Impurity transport calculation by the SIT STRAHL code indicates that the time evolution of the TiK $\alpha$  emission can be explained by neoclassical diffusion and the neoclassical convection, related to the radial electric field and thermal diffusivity. The impurity particle flux

$$\Gamma_j^I = -D_j^I \nabla n_j^I + n_j^I V_j^I \quad (1)$$

consists of the diffusive flux with a neoclassical diffusion coefficient,  $D_j^I$ , and convective term,  $n_j^I V_j^I$ , which is driven by the electric field and thermal force.

$$n_j^I V_j^I = n_j \left\{ D_{1j}^{imp} Z_j \frac{E_r}{T_j} - D_{1j}^{imp} \left( \frac{D_{2j}^{imp}}{D_{1j}^{imp}} - \frac{3}{2} \right) \nabla T \right\} \quad (2)$$

Here  $n_j^I$  denotes the impurity density for each ionization state,  $j$ , of a given impurity species,  $I$ . In general, the

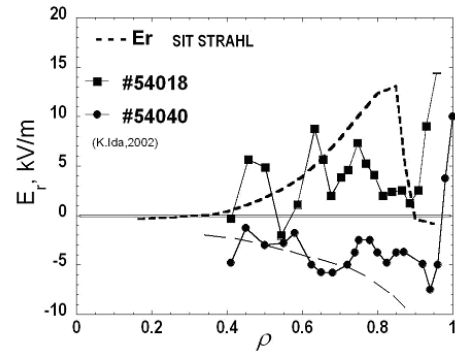


Fig. 2 Radial electric field from CX measurements (at  $t = 1.5$  s) and calculated values (dashed lines) from SIT STRAHL for two LHD discharges with low density  $n(0) = 0.8 \times 10^{19} \text{ m}^{-3}$ , #54018 and with high density  $n(0) = 3.4 \times 10^{19} \text{ m}^{-3}$ , #54040. Impurity impact is negligible (tracer amount). Data are taken from [5, 6].

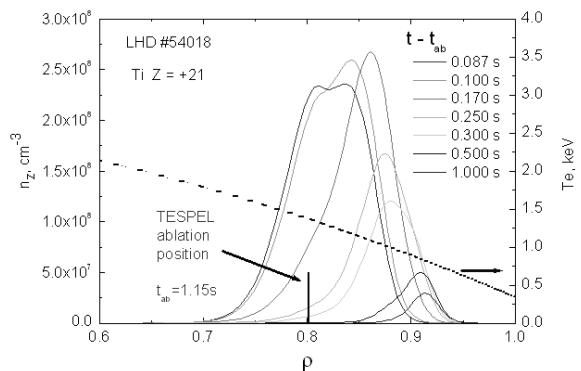


Fig. 3 Radial distribution of Ti Z=21 charge state, plotted in different moments of time after ablation. SIT STRAHL result for LHD discharge (#54018). The ion temperature profile is shown as a dashed line.

diffusion coefficient,  $D_j^I = D_{11,j}^I + D_{an}^I$  includes also the anomalous diffusion. Similarly the anomalous drift velocity,  $V_{an}^I$  can be added to (2) [1, 6]. The radial electric field is calculated from the ambipolarity condition and, in the low density case (shot #54018) is positive over the entire plasma cross-section (see Fig. 2), apart from the central region. For the high density discharge (shot #54040) only an ion root of the ambipolar electric field was found. These results are in qualitative agreement with measurements, done at the plasma edge (see Fig. 2). Calculation show that the last term in (2) has mainly a negative sign because the  $1/\nu$  regime dominates the transport. So that in contrast to tokamaks in axi-symmetric configuration thermal friction brings to the accumulation rather than to the screening of impurities. For Ti ions at 1-2 keV the high charge states  $Z = 21$  and  $Z = 22$  are mainly radiating in the S-X-ray range. Fig. 3 shows the radial distribution of the Ti  $Z = 21$  charge state (which mainly contributes to the SXR signal) in different moments of time. The radial dis-

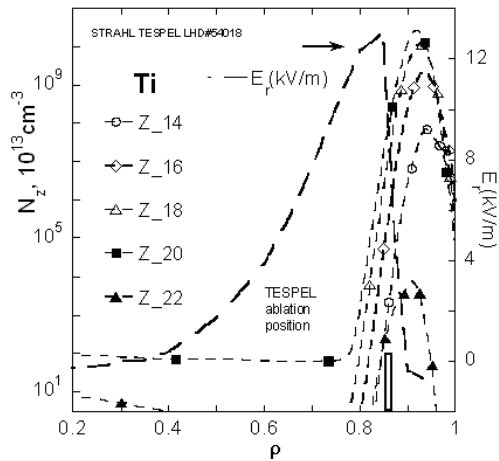


Fig. 4 Radial distribution of highly ionized Ti charge states, plotted at  $t = 2$  sec. Recycling at the wall is taken as zero. SIT STRAHL results for LHD discharge (#54018). The TESPEL pellet deposition is indicated.

tribution of Ti ions of different charge states is governed both by atomic processes and diffusion with convection as well. Fig. 4 shows how highly ionized Ti charge states are radially distributed at  $t = 2$  sec. The main driving force is the electric field, which in this case changes sign near the pellet ablation position (see Fig. 2). Ti ions are pushed by positive electric field outwards and concentrated close to the plasma edge (see Fig. 3 and 4). Fig. 5 shows the radial distribution of impurity flux (1) for high Ti charge states at  $t = 2$  s. The impurity flux at the edge region changes a sign, following the electric field behavior and is remaining outwards directed in the innermost edge region. The neoclassical diffusion coefficient varies over the radius and reaches its maximum of about  $1 \text{ m}^2/\text{s}$  at the center. At the zero flux radial position the impurity concentration reaches its maximum value. Close to the wall impurity ions escaping plasma readily, because of the strong absorption (at the wall the recycling coefficient has been taken as zero).

In the high density case, the  $\text{TiK}\alpha$  emission intensity increase slower than in the low density case (see Fig. 6) and reaches a maximum after about 0.5 s. Then the emission signal drops with a long decay time ( $\tau_{\text{decay}} = 4.1 \text{ s}$ ) up to 3 s, when the NBI heating is turned off. The decay time is closely connected with the impurity confinement time. This indicates that at high density the impurity confinement time is large enough so that impurity ions can accumulate in the core. The long emission decay time in high density discharge is consistent with the fact, that decay time of metallic impurities usually increases with collisionality (see also in [4, 6]). Qualitatively, however, this behavior can not be explained only by neoclassical transport (upper dashed curve in Fig. 6), and additional outward impurity flux is required to reproduce the experimental decay time. Calculation predicts slightly negative radial electric field over most of the radius (see Fig. 2), which agrees

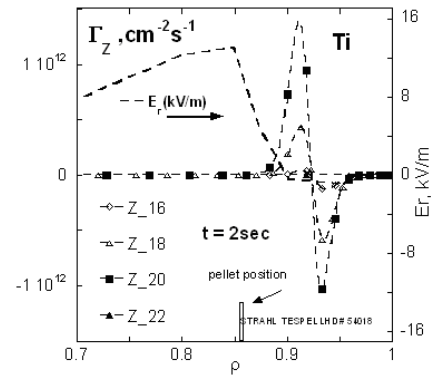


Fig. 5 Radial distribution of impurity flux for high Ti charge states at  $t = 2$  sec. Results from SIT STRAHL calculation; LHD discharge shot #54018, TESPEL injection time 1.2 sec.

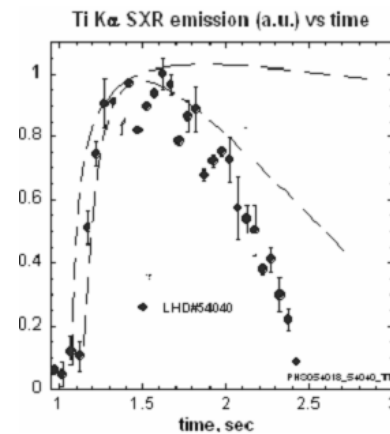


Fig. 6 Time evolution of  $\text{TiK}\alpha$  emission for the LHD discharge (#54040) with high density  $n(0) = 3.4 \times 10^{19} \text{ m}^{-3}$ . The TESPEL pellet with Ti tracer is injected at 1.2 s. The dashed lines show simulation result in the case of purely neoclassical transport (upper line) and in the case of enhanced outward drift (lower dashed line).

with CX measurements. The qualitative agreement can be reached, when anomalous drift velocity is taken (according [6]) proportional to the radial electric field.

In LHD the screening effect of an intrinsically induced  $m/n = 1/1$  magnetic island on impurity behavior has been reported [4]. The experimental plasma profiles show a flattening within the island of about 15 cm width, whereas the measured radial electric field there changes sign within the island [5]. The sheared radial electric field within the island supposedly occurs because the poloidal flow within the island has a different direction in the outer and inner boundaries of the magnetic island and vanishes inside the island. The electric field shear depends not only on the poloidal flow but also on the radial viscosity and the size of the island [5]. The radial profile of the electric field within the magnetic island for the plasma with  $B = 2.83 \text{ T}$  and  $R_{ax} = 3.5 \text{ m}$  has been measured with charge-exchange

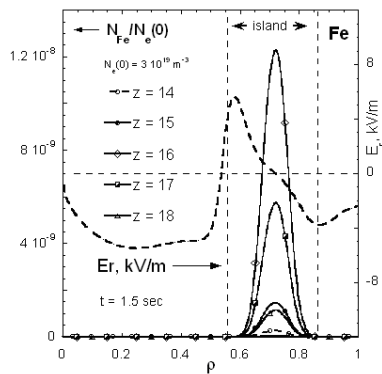


Fig. 7 Fe radial distribution at  $t = 1.5$  s. Dashed line shows the radial electric field. The source at the separatrix ( $\rho = 1$ ) was turned off at  $t = 0.1$  s. Impurities of different charge states are well screened within the island. The island width is  $\sim 15$  cm.

spectroscopy in (see Fig. 4 in [5]) and is shown on Figs. 2, 4, 5 and 7. The corresponding plasma profiles have also been taken from this shot (see Fig. 1 in Ref. [5]). Fig. 7 shows the radial distribution of the Fe charge states at  $t = 1.5$  sec after the source at the wall was turned off. Calculations show that at that time impurity ions are already localized within the island. The different sign of the electric field in the outermost and the innermost parts of the island brings about an effective “pumping” of impurity ions into the island from the plasma edge and their screening from penetration into the bulk plasma. Eventually, when the impurity concentration grows within the island the diffusive flux increases and can overcome the screening effect of the positive electric field. This can explain a possible slow penetration of impurities toward the center. This can readily happen in the case of light impurities. In the case of Fe the diffusion coefficients are smaller and ions are better confined within the island [7]. It is also shown that in the bulk plasma a noticeable decay of the inward convective flux takes place due to a flattening of the plasma profiles. The total impurity flux turns in time to zero, as it should be in a steady stable condition. The convection within the outermost part of the island is competing with

the diffusion. This brings about a sharp increase in impurity concentration within the island, where the electric field goes through zero. This process stops once inward diffusion overcomes the electric field and the light impurities can penetrate through the electric field barrier and finally accumulate in the center. In the case of Fe ions the steady state was achieved within 1.5 s, after which the spatial distribution does not change. The impurity ions are well retained within the island. The total flux is zero; however, the fluxes of partial charge states are still slowly relaxing to zero.

### 3. Conclusions

The preliminary results of modeling of the TESPEL signal by using the SIT STRAHL code are presented. The reconstruction of the SXR emission in the case of a low density discharge can be done in the frame of neoclassical theory. In the case of high density, the negative electric field effect must be compensated by additional (anomalous) outwards convection. Calculation show that in contrast to tokamaks in a non-axi symmetric configuration thermal friction has an opposite sign. The radial electric field plays a dominant role in the accumulation of impurity ions. Only in the case of low density and/or high temperature (positive radial electric field) can one expect impurity retention at the plasma edge. It is shown, that impurity ions can be retained within an externally induced magnetic island  $m/n = 1/1$  at the edge of LHD. This occurs due to a positive electric field in the innermost part of an island.

This work is supported by a budgetary Grant-in-Aid No.NIFS06ULHH001-4 and NIFS05ULHH510 of the National Institute for Fusion Science.

- [1] P. Goncharov *et al.*, Stellarator Impurity STRAHL code development in NIFS, ITC-16, P13-07.
- [2] S. Sudo *et al.*, J. Plasma Fusion Res. **69**, 1349 (1993).
- [3] K. Behringer, JET Report JET-R (87) 08, JET (1987).
- [4] Y. Nakamura *et al.*, Nucl. Fusion **43**, 219 (2003).
- [5] K. Ida *et al.*, Phys. Rev. Lett. **88**, 015002 (2002); **86**, 5297 (2001); Phys. Plasma **8**, 1 (2001).
- [6] D. Kalinina, Ph.D. Dissertation, Grad. Univ. Advanced Studies (2005).
- [7] Yu. Igitkhanov *et al.*, Fusion Sci. Technol. **50**, 268 (2006).